Efficiency of Amptek XR-100T-CdTe and -CZT Detectors
Application Note ANCZT-1 Rev 2.

Bob Redus, December 13, 2002

Amptek's XR-100T-CdTe and -CZT are high performance x-ray and gamma ray detector systems. In both systems, a detector element and preamplifier components are mounted on a thermoelectric cooler. These products use wide bandgap, compound semiconductors as the detector element. Amptek used conventional $CdZn_xTe_{1-x}$ (CZT) detectors for several years, but in the past year has been using CdTe PIN diodes as detectors. The CdTe PIN diodes provide significantly improved spectral performance, through better charge transport properties and reduced leakage currents. Many aspects of these devices are discussed in an accompanying Amptek Application Note, Charge Trapping in CdTe/CZT detectors (ANCZT-2).

An important consideration is often the detection efficiency of these detectors. Due to charge transport effects, defining the detection efficiency is somewhat subtle. The purpose of this note is to provide general information on efficiency, for estimating system performance, and to recommend procedures for measuring the actual efficiency of a given detector.

1 INTRODUCTION

As is well known[i], when a beam of energetic photons, X-rays or γ-rays, passes through a material the result is a simple exponential attenuation of the primary beam. Each of the possible interaction processes can be characterized by a probability of occurrence per unit path length in the absorber. The sum of the probabilities for the individual processes is the total probability per unit length that the photon is removed from the beam. This is termed the linear attenuation coefficient, is denoted μ, and has units of inverse length (cm^{-1}). The number of primary photons transmitted through a thickness t is

$$I_{trans} = I_0 e^{-mt}$$

where I_0 is the flux of incident photons, t is the thickness of the attenuator, μ is the linear attenuation coefficient, and I_{trans} is the flux of transmitted primary photons. The number of primary photons interacting in a thickness t is obviously

$$I_{in} = I_0 \left[1 - e^{-mt}\right]$$

The linear attenuation coefficient obviously depends strongly on energy, since the interaction mechanisms are energy dependent. The attenuation is often described using the mass attenuation coefficient, $\mu_m = \mu/\rho$ where ρ is the density of the medium. This can be written in units of cm^2/g, with the density in g/cm^3, or in units of barns (1 barn = 10^{-24} cm^2) with the density in atoms per cm^3.

There are several different processes by which photons interact. In the energy range most often measured with the XR-100T-CdTe or -CZT, the most important processes are the photoelectric interaction and Compton scattering. In a photoelectric interaction, the entire incident energy of the interacting photon is deposited in the detector, while in Compton scattering, only a portion of the incident energy will generally be deposited in the detector. Photoelectric interactions contribute to the full energy, which is usually of primary interest. The probability of a photoelectric interaction is usually of primary interest.

2 APPLICATION TO THE XR-100T-CDTE/CZT

Amptek's standard XR-100T-CdTe consists of a 1 mm thick CdTe detector located behind a 10 mil Be window. The older CZT detectors were typically 2 mm thick, also behind a 10 mil Be window. The Zn fraction of the CZT is typically 0.1. For both, the probability of a photon interaction somewhere in the detector thickness is the product of (1) the probability of transmission through Be and (2) the probability of interaction in the material,

$$P = \left(e^{-m_{Be} t_{Be}}\right)\left(1 - e^{-m_{CZT} t_{CZT}}\right)$$

The attenuation coefficients can be obtained through a variety of tables or through commercially available software[ii]. Table 1 lists attenuation coefficients at roughly log-spaced energy intervals from 1 keV to 10 MeV. It also lists the probability of an interaction occurring in the 2 mm physical thickness of CZT.

Table 2 provides the same information for the new 1 mm thick CdTe. The probability calculation includes the effects of transmission through the Be window and of stopping in the detector, but neglect the effects of trapping and hole tailing. Both total and photoelectric probabilities are given. Plots of the interaction probabilities are shown in Figure 1 and Figure 2 for the 2 mm CZT and Figures 3 and 4 for the 1 mm CdTe. A linear interpolation between the tabulated values is generally valid at low energies, with a log-log interpolation more accurate at high energies.

	Probability in 2 mm CZT		Linear Attenuation (cm^{-1})	
Energy (keV)	Total Interaction	Photoelectric Interaction	Total	Photoelectric
1	0.00%	0.00%	4.82E+04	4.82E+04
1.006	0.00%	0.00%	4.76E+04	4.76E+04
1.006001	0.00%	0.00%	4.88E+04	4.87E+04
1.5	0.02%	0.02%	2.08E+04	2.07E+04
2	2.99%	2.99%	1.05E+04	1.05E+04
3	36.80%	36.80%	3.87E+03	3.83E+03
3.5375	52.76%	52.76%	2.55E+03	2.52E+03
3.537501	52.76%	52.76%	4.67E+03	4.64E+03
3.727	58.39%	58.39%	4.11E+03	4.07E+03
3.727001	58.39%	58.39%	5.11E+03	5.07E+03
4	66.49%	66.49%	4.29E+03	4.26E+03
4.018	66.76%	66.76%	4.24E+03	4.21E+03
4.018001	66.76%	66.76%	4.70E+03	4.66E+03
4.3414	71.60%	71.60%	3.87E+03	3.84E+03
4.341401	71.60%	71.60%	5.62E+03	5.59E+03
4.612	75.64%	75.64%	4.90E+03	4.87E+03
4.612001	75.64%	75.64%	5.73E+03	5.70E+03
4.9392	80.53%	80.53%	4.86E+03	4.83E+03
4.939201	80.53%	80.53%	5.27E+03	5.25E+03
5	81.44%	81.44%	5.12E+03	5.09E+03
6	88.80%	88.80%	3.22E+03	3.20E+03
8	94.86%	94.86%	1.52E+03	1.50E+03
10	97.01%	97.01%	8.76E+02	8.60E+02
12	97.79%	97.79%	5.38E+02	5.23E+02
15	98.57%	98.57%	2.96E+02	2.85E+02
20	98.95%	98.95%	1.36E+02	1.28E+02
25	98.95%	98.95%	7.47E+01	6.85E+01
26.711	99.09%	99.09%	6.25E+01	5.69E+01
26.71101	99.09%	99.09%	1.74E+02	1.68E+02
30	99.16%	99.16%	1.29E+02	1.24E+02
31.814	99.16%	99.16%	1.11E+02	1.06E+02
31.81401	99.16%	99.16%	2.13E+02	2.08E+02
35	99.16%	99.16%	1.66E+02	1.62E+02

	Probability in 2 mm CZT		Linear Attenuation (cm^{-1})	
Energy (keV)	Total Interaction	Photoelectric Interaction	Total	Photoelectric
40	99.23%	99.23%	1.18E+02	1.14E+02
45	99.23%	99.23%	8.61E+01	8.31E+01
50	99.27%	99.27%	6.51E+01	6.24E+01
55	99.27%	99.27%	5.04E+01	4.80E+01
60	99.27%	99.25%	3.99E+01	3.78E+01
70	98.79%	98.56%	2.64E+01	2.45E+01
80	96.85%	95.92%	1.84E+01	1.68E+01
90	92.65%	90.40%	1.35E+01	1.20E+01
100	86.46%	82.68%	1.02E+01	8.92E+00
125	68.54%	60.52%	5.85E+00	4.69E+00
150	52.14%	42.40%	3.71E+00	2.78E+00
175	41.01%	29.84%	2.66E+00	1.78E+00
200	32.67%	21.47%	1.99E+00	1.22E+00
250	23.76%	12.09%	1.36E+00	6.48E-01
300	18.09%	7.42%	1.00E+00	3.87E-01
350	15.27%	4.95%	8.32E-01	2.55E-01
400	13.16%	3.48%	7.08E-01	1.78E-01
500	10.82%	1.97%	5.75E-01	1.00E-01
600	9.45%	1.27%	4.98E-01	6.39E-02
800	7.83%	0.66%	4.09E-01	3.31E-02
1000	6.86%	0.41%	3.56E-01	2.06E-02
1022	6.78%	0.39%	3.51E-01	1.96E-02
1250	6.06%	0.26%	3.13E-01	1.32E-02
1500	5.53%	0.19%	2.85E-01	9.49E-03
2000	4.92%	0.12%	2.52E-01	5.78E-03
3000	4.42%	0.06%	2.26E-01	3.07E-03
4000	4.26%	0.04%	2.18E-01	2.04E-03
5000	4.25%	0.03%	2.17E-01	1.51E-03
6000	4.29%	0.02%	2.19E-01	1.19E-03
7000	4.36%	0.02%	2.23E-01	9.81E-04
8000	4.45%	0.02%	2.28E-01	8.33E-04
9000	4.54%	0.01%	2.33E-01	7.22E-04
10000	4.64%	0.01%	2.38E-01	6.38E-04

Table 1. Table of linear attenuation coefficients for CZT, along with interaction probabilities for the 2 mm CZT thickness. This table does not reflect the effective depth due to hole tailing, as discussed in the text.

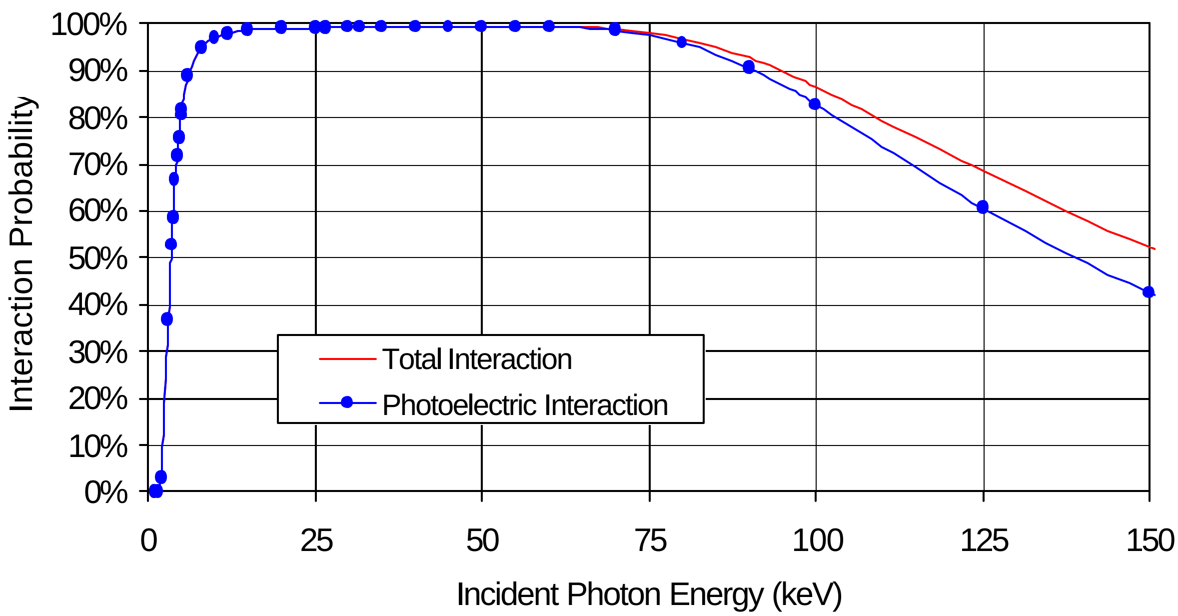

Figure 1. Linear plot of interaction probability over the lower energy range.

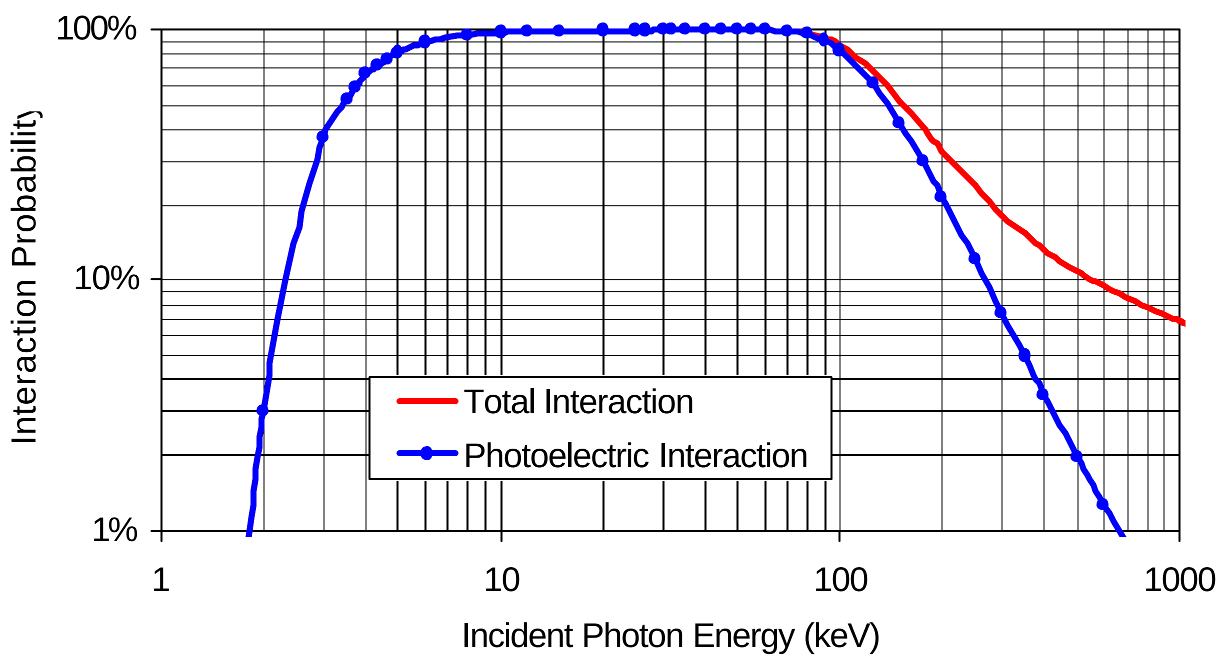

Figure 2. Log-log plot of interaction probability between 1 keV and 1 MeV.

Probability in 1 mm CdTe			Linear Attenuation (cm-1)	
Energy (keV)	Total Interaction	Photoelectric Interaction	Total	Photoelectric
1	0.00%	0.00%	4.82E+04	4.82E+04
1.006	0.00%	0.00%	4.76E+04	4.76E+04
1.006001	0.00%	0.00%	4.88E+04	4.87E+04
1.5	0.02%	0.02%	2.08E+04	2.07E+04
2	2.99%	2.99%	1.05E+04	1.05E+04
3	36.80%	36.80%	3.87E+03	3.83E+03
3.5375	52.76%	52.76%	2.55E+03	2.52E+03
3.537501	52.76%	52.76%	4.67E+03	4.64E+03
3.727	58.39%	58.39%	4.11E+03	4.07E+03
3.727001	58.39%	58.39%	5.11E+03	5.07E+03
4	66.49%	66.49%	4.29E+03	4.26E+03
4.018	66.76%	66.76%	4.24E+03	4.21E+03
4.018001	66.76%	66.76%	4.70E+03	4.66E+03
4.3414	71.60%	71.60%	3.87E+03	3.84E+03
4.341401	71.60%	71.60%	5.62E+03	5.59E+03
4.612	75.64%	75.64%	4.90E+03	4.87E+03
4.612001	75.64%	75.64%	5.73E+03	5.70E+03
4.9392	80.53%	80.53%	4.86E+03	4.83E+03
4.939201	80.53%	80.53%	5.27E+03	5.25E+03
5	81.44%	81.44%	5.12E+03	5.09E+03
6	88.80%	88.80%	3.22E+03	3.20E+03
8	94.86%	94.86%	1.52E+03	1.50E+03
10	97.01%	97.01%	8.76E+02	8.60E+02
12	97.79%	97.79%	5.38E+02	5.23E+02
15	98.57%	98.57%	2.96E+02	2.85E+02
20	98.95%	98.95%	1.36E+02	1.28E+02
25	98.89%	98.84%	7.47E+01	6.85E+01
26.711	98.90%	98.75%	6.25E+01	5.69E+01
26.71101	99.09%	99.09%	1.74E+02	1.68E+02
30	99.16%	99.16%	1.29E+02	1.24E+02
31.814	99.16%	99.16%	1.11E+02	1.06E+02
31.81401	99.16%	99.16%	2.13E+02	2.08E+02
35	99.16%	99.16%	1.66E+02	1.62E+02
40	99.23%	99.23%	1.18E+02	1.14E+02
45	99.21%	99.21%	8.61E+01	8.31E+01
50	99.12%	99.08%	6.51E+01	6.24E+01
55	98.63%	98.46%	5.04E+01	4.80E+01
60	97.47%	97.03%	3.99E+01	3.78E+01
70	92.20%	90.73%	2.64E+01	2.45E+01
80	83.60%	80.90%	1.84E+01	1.68E+01
90	73.55%	69.54%	1.35E+01	1.20E+01
100	63.55%	58.64%	1.02E+01	8.92E+00
125	44.02%	37.23%	5.85E+00	4.69E+00
150	30.85%	24.13%	3.71E+00	2.78E+00
175	23.22%	16.25%	2.66E+00	1.78E+00
200	17.96%	11.38%	1.99E+00	1.22E+00
250	12.69%	6.24%	1.36E+00	6.48E-01
300	9.50%	3.78%	1.00E+00	3.87E-01
350	7.95%	2.51%	8.32E-01	2.55E-01
400	6.81%	1.76%	7.08E-01	1.78E-01
500	5.56%	0.99%	5.75E-01	1.00E-01
600	4.84%	0.64%	4.98E-01	6.39E-02
800	4.00%	0.33%	4.09E-01	3.31E-02
1000	3.49%	0.21%	3.56E-01	2.06E-02
1022	3.45%	0.20%	3.51E-01	1.96E-02
1250	3.08%	0.13%	3.13E-01	1.32E-02
1500	2.80%	0.09%	2.85E-01	9.49E-03
2000	2.49%	0.06%	2.52E-01	5.78E-03
3000	2.23%	0.03%	2.26E-01	3.07E-03
4000	2.16%	0.02%	2.18E-01	2.04E-03
5000	2.15%	0.02%	2.17E-01	1.51E-03
6000	2.17%	0.01%	2.19E-01	1.19E-03
7000	2.20%	0.01%	2.23E-01	9.81E-04
8000	2.25%	0.01%	2.28E-01	8.33E-04
9000	2.30%	0.01%	2.33E-01	7.22E-04
10000	2.35%	0.01%	2.38E-01	6.38E-04

Table 2. Table of linear attenuation coefficients for CdTe, along with interaction probabilities for the 1 mm CdTe thickness. This table does not reflect the effective depth due to hole tailing, as discussed in the text.

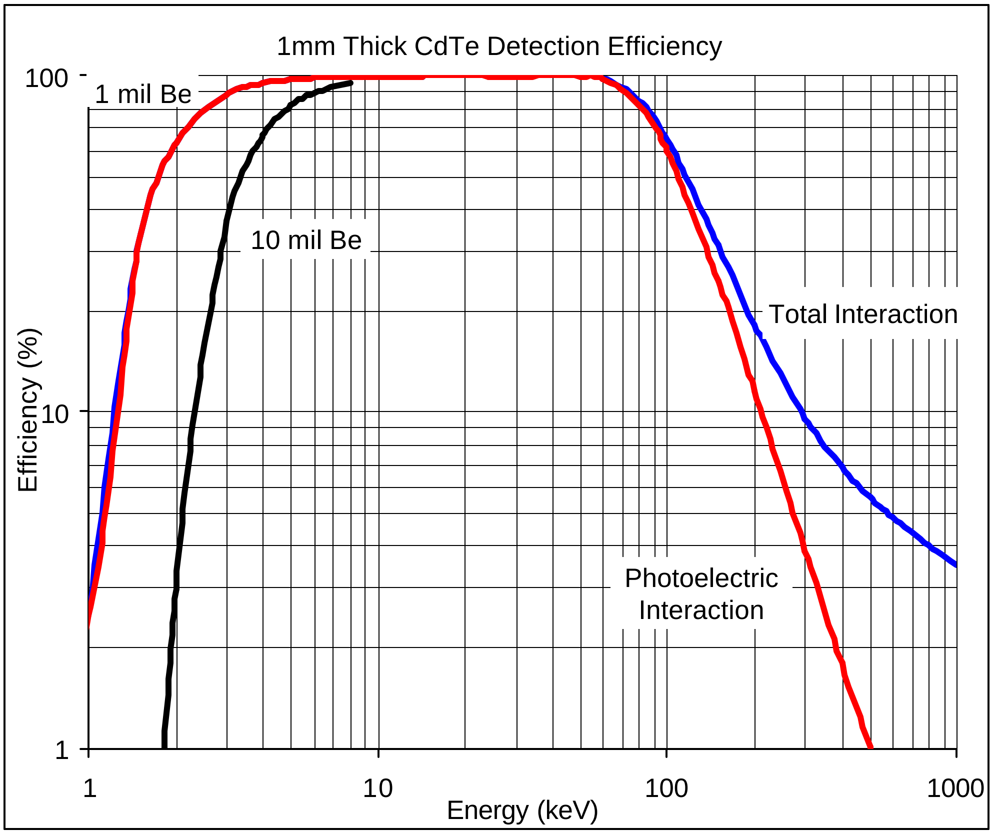

Figure 4. Log-log plot of interaction probability between 1 keV and 1 MeV for 1 mm CdTe.

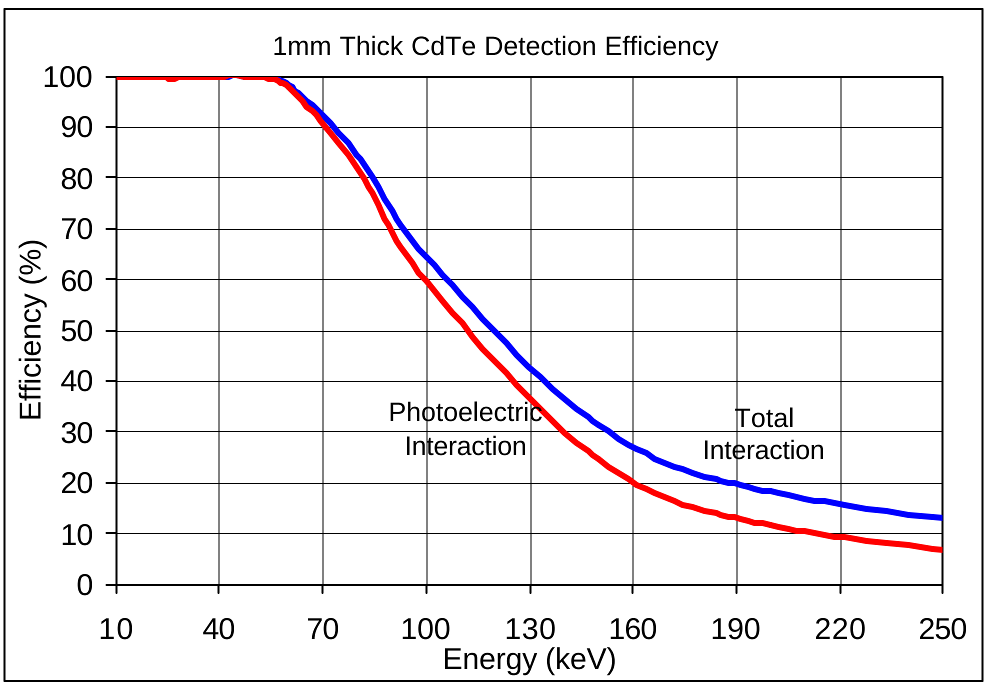

Figure 5. Linear plot of interaction probability over the lower energy range for 1 mm CdTe.

3 CONSEQUENCES OF TRAPPING AND HOLE TAILING

Both CdTe and CZT are wide bandgap, high-Z, compound semiconductor materials. They are used for X-ray and γ-ray spectroscopy because they have a very high linear attenuation coefficient, permitting high efficiency in a small volume, and low leakage currents, permitting low electronic noise without cryogenic cooling[iii]. However, like other compound semiconductors, they exhibit significant spectral distortions due to hole trapping. As is discussed elsewhere[iv], the trapping length of holes in CdTe and CZT is smaller than the linear dimensions of the detector. For interaction occurring near the anode, virtually all of the signal is due to electrons and so the full charge is collected. For interactions occurring near the cathode, virtually all of the signal is due to holes and so a smaller charge is collected.

The result is that the measured signal, the measured "energy", depends upon the depth of the interaction on the detector, decreasing with increasing depth. In the output spectrum, one observes a tail of counts towards lower amplitudes, an effect known as "hole tailing". Figure 5 is a plot of the pulse height as a function of depth in the detector, computed from the Hecht[v] relation for two different values for the hole lifetime. Figure 6 is a plot of a measured spectrum demonstrating hole tailing with a 2 mm CZT detector. This was a measurement of a ^{57}Co source, which emits primarily at 122 keV. The blue trace in Figure 6 is the raw spectrum. The tail of counts extending to low values is due to hole tailing.

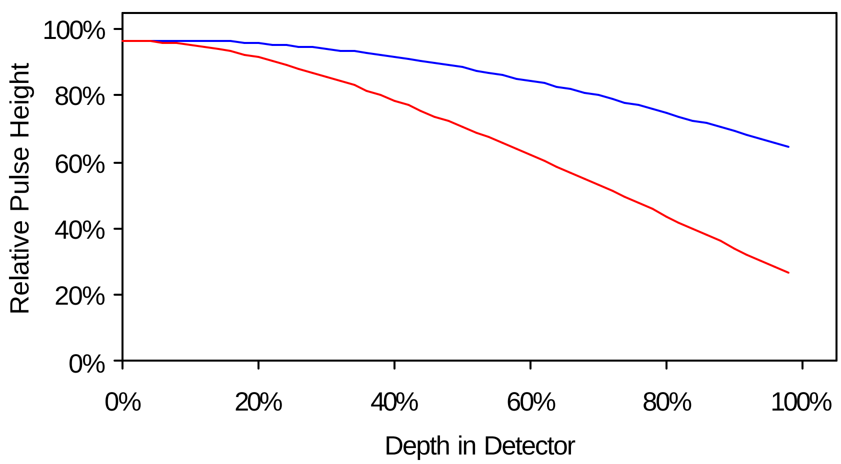

Figure 5. Plot showing the induced signal size as a function of depth, computed for two different values of the hole lifetime.

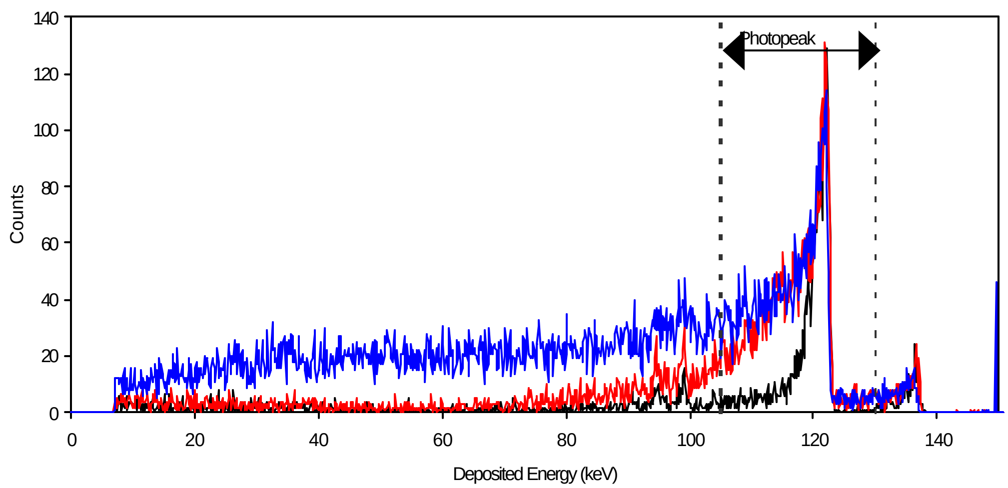

Figure 6. Measured ^{57}Co spectra, obtained with an Amptek's XR-100T-CZT. The blue trace shows the raw data, with hole tailing down to low amplitudes. The red and black traces show the result of applying risetime discrimination. The resolution is improved, but the efficiency is lower than that expected from the physical dimensions of the detector.

Note that in Figure 5, for the blue curve, about 40% of the depth of the detector produces a full signal. The rest of the depth produces a smaller signal. The effective volume of the detector, which contributes to the primary, full energy peak, is only 40% of the physical volume of the detector. For the red curve, about 20% of the detector volume contributes to the full energy peak.

For CdTe, CZT, and other detectors in which charge trapping is important, it is critical to distinguish between the total geometric efficiency and the efficiency of the full energy peak. The total geometric efficiency, which is due to the total physical volume of the detector, can be used to compute the total rate of counts in the detector. The efficiency of the full energy peak, which is due to the volume of the detector leading to “full charge collection”, can be used to compute the total rate of counts in the primary peak. The phrase “full charge collection” is in quotation marks because it is not well defined. The charge collection efficiency decreases smoothly with increasing depth. Different users may define the full energy peak differently, depending on the specific application.

In Amptek’s XR-100T-CdTe/CZT, risetime discrimination (RTD) is used to minimize spectral distortions due to hole tailing. Figure 5 showed that the induced signal size is correlated with depth in the detector. The risetime of the pulse from the preamp is also well correlated with depth in the detector. Therefore, Amptek’s PX2-CZT measures the risetime of the pulses and rejects those with a long risetime. This leads to a significant improvement in the quality of the spectrum, as can be seen in Figure 6. The red and black traces show the effects of two different RTD thresholds. The black trace provides the very highest resolution, while the red trace shows somewhat poorer resolution but higher efficiency. The RTD setting for the red trace was set to maximize the efficiency for a given definition of the ^{57}Co photopeak region[vi].

When RTD is used with the XR-100T-CZT, the detection efficiency is significantly lower than would be anticipated from the physical dimensions of the detector. The effective depth depends upon the charge transport properties of the material. These are not well controlled by the manufacturer, so significant variations exist from one detector to the next. The effective depth also depends upon the RTD setting. The effective depth of Amptek’s XR-100T-CZT (2 mm thick CZT) detectors is commonly in the range of 0.5 to 1 mm, so is one quarter to one half of the physical depth.

For the new 1 mm thick CdTe detectors, RTD is not as necessary. This is due to the improved charge transport of the device (see application note ANCZT 2). Figure 7 is a plot of a CdTe detector with RTD on and off for ^{57}Co. Note the improvement over the 2 mm CZT from Figure 6.

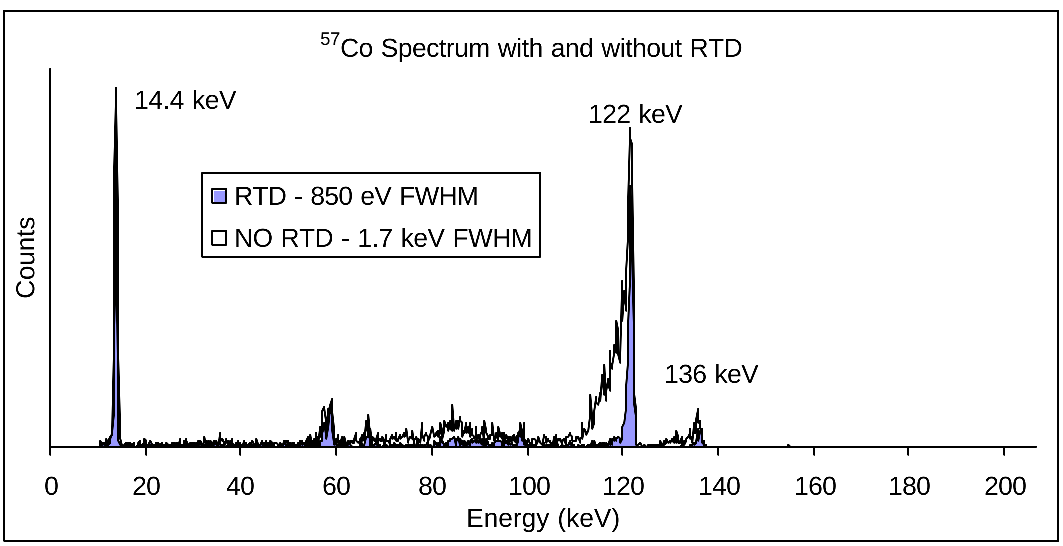

Figure 7. ^{57}Co spectrum with RTD on and off for the 1 mm thick CdTe.

4 MEASURING THE EFFICIENCY

In many applications it is important to know the detection efficiency at a particular energy. Because there exists a wide variation in the effective depth of Amptek’s XR-100T-CZT and -CdTe detectors, if a user requires precise knowledge, the best solution is to measure the actual efficiency at the energy of interest from some well-known standard. Since this can be difficult, another approach is to measure the effective depth of the particular detector. There are two approaches to this measurement.

If one has a calibrated source, with a very well known strength and an energy high enough to be only partially absorbed in the detector material, then the effective depth can be readily computed by inverting the relation above:

$$P = 1 - e^{-mt} \Rightarrow t = -\ln(1 - P)/m$$

For example, from Figure 1 the 122 keV line from ^{57}Co should be detected with 70% efficiency and from Table 1 that the linear attenuation coefficient is 6.22 cm^{-1}. Assume that a lab measurement shows that this line is detected with 35% efficiency. This gives t=0.7 mm. This effective depth can be used to computed the efficiency at any other energy (above the energy where attenuation in the Be window is significant).

In the absence of a calibrated source, then a single source which emits γ-rays at two distinct lines with a well known ratio can be used, if at least one of the lines is high enough in energy to be detected with <100% efficiency and both are above the energy where the Be window is significant. The source must not attenuate either line significantly. For example, ^{57}Co emits at 14.4 keV with 9.8% efficiency and 122 keV with 85.6% efficiency. We define P_1 and P_2 as the probabilities of emission of the two lines, N_1 and N_2 and the measured counts of the two lines, and μ_1 and μ_2 are the linear attenuation coefficients of the two lines. The ratio of the measured counts will obviously be

$$\frac{N_1}{N_2} = \frac{P_1\left(1 - e^{-m_1 t}\right)}{P_2\left(1 - e^{-m_{21} t}\right)}$$

Applying some algebra, this implies

$$t = \frac{\ln(N_1 P_2 - N_2 P_1) - [\ln(N_1 P_2) - \ln(N_2 P)]}{(m_1 - m_2)}$$

[i] a) Knoll, Glenn F., Radiation Detection and Measurement, John Wiley & Sons, New York. 1989.

b) Tsoulfanidis, Nicholas, Measurement and Detection of Radiation, Hemphire Publishing Corporation, New York, 1983.

[ii] Photcoeff by AIC Software Inc. http://www.photcoef.com provides tables/graphs/data on coefficients.

[iii] Jordanov, V.T., J.A. Pantazis, and A.C. Huber, "Thermoelectrically-Cooled Cadmium Zinc Telluride Detectors (CZT) for X-Ray and Gamma-Ray Detection," Radiation, Vol. 43, No. 1, July 1996.

[iv] a) Charge Trapping in XR-100T-CdTe/CZT Detectors, Amptek Application Note (ANCZT-2) by Bob Redus, 2002.

b) Semiconductors and Semimetals vol. 43, Semiconductors for Room Temperature Nuclear Detector Applications, section on Characterization and Quantification of Detector Performance by Vernon M. Gerrish, Volume Editors T.E. Schlesinger and R.B James, Academic Press, San Diego, 1995.

[v] a) Hecht (1932)

b) Semiconductors and Semimetals vol. 43, Semiconductors for Room Temperature Nuclear Detector Applications, section on Characterization and Quantification of Detector Performance by Vernon M. Gerrish discusses Hecht relation, Volume Editors T.E. Schlesinger and R.B James, Academic Press, San Diego, 1995.

[vi] Squillante, M.R., Presentation at 11th International Workshop on Room Temperature Semiconductor X-Ray and Gamma-Ray Detectors and Associated Electronics, 1999 Vienna Austria.